

PACS numbers: 42.81.Bm; 42.81.Gs; 42.81.Pa; 85.70.Sq
DOI: 10.1070/QE2009v039n11ABEH014149

Spun microstructured optical fibres for Faraday effect current sensors

Yu.K. Chamorovsky, N.I. Starostin, S.K. Morshnev,
V.P. Gubin, M.V. Ryabko, A.I. Sazonov, I.L. Vorob'ev

***Abstract*. We report a simple design of spun holey fibres and the first experimental study of the magneto-optical response of spun microstructured fibres with high built-in birefringence. Such fibres enable the Faraday-effect-induced phase shift to effectively accumulate in a magnetic field even at very small coiling diameters. For example, the magneto-optical sensitivity of a 5-mm-diameter fibre coil consisting of 100 turns is $\sim 70\,\%$ that of an ideal fibre, in good agreement with theoretical predictions.**

Keywords: *microstructured fibre, spun fibre, Faraday effect, current sensor.*

Microstructured optical fibres (MOFs) possess a number of characteristics that make them rather attractive for application in fibreoptic sensors of physical quantities. In particular, polarisation-maintaining MOFs offer the advantages of very low bending losses and excellent temperature stability of their birefringence (BR) [1, 2]. In this paper, we examine one more unique property of MOFs and its possible practical application in Faraday effect current sensors. As shown earlier [3 – 5], one of the most promising types of fibres for current-sensing applications is spun fibre, which is fabricated by spinning preforms with a built-in linear BR (beat length, L_b) during the drawing process. Spun fibres have a helical structure of the built-in linear BR axes, with a spin pitch L_{tw}. Such fibres are stable to external mechanical stresses and retain high magneto-optical sensitivity down to very small bending radii, ~ 30 mm [3, 5]. Conventional spun fibres typically have $L_b > L_{tw}$. Spin pitches $L_{tw} < 1$ mm are technically difficult to produce, whereas MOFs are characterised by a high built-in linear BR: $L_b < 1$ mm. For this reason, spun MOFs typically have the inverse relationship: $L_b < L_{tw}$.

Fibre bending with radius R induces an additional linear BR with a beat length [6]

$$L_{ind} = 22.792\,\frac{\lambda}{n_0^3}\,\frac{R^2}{r^2}, \tag{1}$$

where r is the outer fibre radius; n_0 is the refractive index of silica; and λ is the working wavelength.

The polarisation state (PS) of light propagating through a fibre can be determined using a differential matrix N:

$$\begin{vmatrix} dE_R/dz \\ dE_L/dz \end{vmatrix} = \begin{Vmatrix} N_{11} & N_{12} \\ N_{21} & N_{22} \end{Vmatrix} \begin{vmatrix} E_R \\ E_L \end{vmatrix}, \tag{2}$$

where E_R and E_L are the right-hand and left-hand circularly polarised field components. In a circular polarisation basis, the differential matrix for a fibre with a helical structure of its linear BR axes that is bent with radius R and placed in a magnetic field has the form [5]

$$N = \begin{Vmatrix} \pm i\gamma & i\,\dfrac{\Delta\beta}{2}\exp(i2\xi z) + i\,\dfrac{\delta}{2}\exp(i2\varphi_0) \\ i\,\dfrac{\Delta\beta}{2}\exp(-i2\xi z) + i\,\dfrac{\delta}{2}\exp(-i2\varphi_0) & \mp i\gamma \end{Vmatrix}. \tag{3}$$

Here, $\Delta\beta = 2\pi/L_b$ is the rate of the increase in the phase delay due to the built-in linear BR for waves with orthogonal linear polarisations; $\xi = 2\pi/L_{tw}$ is the rate of the increase in the rotation angle of the BR axes with increasing fibre length; $\delta = 2\pi/L_{ind}$ is the rate of the increase in the phase delay due to the bend-induced linear BR; φ_0 is the angle between the bend-induced and built-in linear BR axes;

$$\gamma = VB_z = 2\pi/L_F \tag{4}$$

is the rate of the increase in the Faraday-effect-induced phase delay between waves with two orthogonal circular polarisations, E_R and E_L; B_z is the magnetic field along the fibre; V is the Verdet constant of silica; and L_F is the beat length of the Faraday-effect-induced circular BR.

Since (2) with matrix (3) cannot be integrated by quadratures, it was solved numerically using computational techniques described elsewhere [5]. To illustrate computation results, one typically resorts to the Poincare sphere representation. We find the complex-valued electric components E_x and E_y of the wave and then the corresponding point χ in the complex plane:

$$\chi = E_y/E_x. \tag{5}$$

As shown previously [7], the complex plane with points defined by (5) is a map of the Poincare sphere. Its equator projects onto the real axis of the complex plane, and the points on the equator represent linear polarisations. In

Yu.K. Chamorovsky, N.I. Starostin, S.K. Morshnev, V.P. Gubin, M.V. Ryabko, A.I. Sazonov, I.L. Vorob'ev V.A. Kotel'nikov Institute of Radio Engineering and Electronics (Fryazino Branch), Russian Academy of Sciences, pl. Akad. Vvedenskogo 1, 141190 Fryazino, Moscow region, Russia; e-mail: yuchamor@tochka.ru, nis229@ire216.msk.su

Received 7 May 2009; revision received 17 July 2009
Kvantovaya Elektronika **39** (11) 1074 – 1077 (2009)
Translated by O.M. Tsarev

particular, the point $\chi = \{0, 0\}$ corresponds to the $\boldsymbol{E}||x$ linear polarisation, and $\chi = \{\infty, \infty\}$ corresponds to the $\boldsymbol{E}||y$ linear polarisation. The poles of the Poincare sphere (circular states) project onto the points $\chi = \{0, \mathrm{i}\}$ (right-hand circular polarisation) and $\chi = \{0, -\mathrm{i}\}$ (left-hand circular polarisation). The upper and lower half-planes correspond to right-hand and left-hand elliptically polarised states, respectively.

In magnetic field (electric current) sensors based on the Faraday effect, two waves with orthogonal circular polarisations pass through a sensing element in the form of a magnetic-field-sensitive optical fibre. The magnetic field produces a phase difference between the waves, which is measured by a linear reflective interferometer [5, 8] in which all the phase differences between the orthogonally polarised waves are compensated except for that due to the Faraday effect. In our model, we examine the PS evolution of circularly polarised waves. Any deviation from a purely circular polarisation reduces the magneto-optical response of the interferometer. The reason for this is that any elliptical PS can be represented as a sum of two orthogonal circular polarisations with different weights and phases, which obviously make opposite contributions to the Faraday-effect-induced phase delay.

Calculating the complex-valued electric components of the circularly polarised modes, one can easily determine the Faraday-effect-induced phase difference between the modes, S, and the relative magneto-optical sensitivity of the coil, S/S_{id}, where S_{id} is the phase difference between the circularly polarised modes in an ideal (isotropic) fibre.

Figure 1 illustrates the PS evolution in a fibre coil of radius $R = 6$ mm with a helical structure of linear BR at a spin pitch $L_{\mathrm{tw}} = 3$ mm and different built-in linear BR beat lengths, L_{b} (right-hand circular polarisation at the fibre input).

In Fig. 1a, the PS evolution resembles the motion of the tip of a gyroscope. The nutation loops touch an envelope circle like in the case of precession. As shown earlier [5, 9], the radius of the precession envelope ρ_{p} depends on the bending radius R: with decreasing R, ρ_{p} increases and the sensitivity of the coil diminishes. It can be seen in Fig. 1a that the built-in linear BR ($L_{\mathrm{b}} = 10$ mm) cannot suppress the bend-induced BR ($L_{\mathrm{ind}} = 108$ mm), the PS passes to the southern hemisphere, and the sensitivity drops to 0.3.

The nutation amplitude A_{nut} depends on the $L_{\mathrm{tw}}/L_{\mathrm{b}}$ ratio [5, 9]: the larger this ratio (the higher the built-in linear BR), the greater the A_{nut} value and the lower the sensitivity of the coil. As seen in Fig. 1b, increasing the built-in linear BR (reducing the L_{b}) decreases the precession radius ρ_{p} and concurrently increases the nutation amplitude A_{nut}. The high built-in linear BR suppresses the bend-induced linear BR, but here the sensitivity is determined by the ratio $L_{\mathrm{tw}}/L_{\mathrm{b}} = 1$ ($S/S_{\mathrm{id}} = 0.74$). At a still higher built-in linear BR (Fig. 1c), the helical structure cannot suppress it, and the A_{nut} amplitude is so large that the PS again reaches the southern hemisphere of the Poincare sphere, and the sensitivity of the coil, S/S_{id}, drops to 0.3. Here, we have the relationship $L_{\mathrm{b}} < L_{\mathrm{tw}}$, typical of spun MOFs [10]. According to theoretical concepts [3, 5, 10], this would be expected to markedly reduce the response.

It should be emphasised that, in our computations, radiation launched into the fibre coil was assumed to be circularly polarised. In the case of conventional fibres, with $L_{\mathrm{b}} > L_{\mathrm{tw}}$, such radiation ensures the highest sensitivity. Our results show that, with the inverse relationship ($L_{\mathrm{b}} < L_{\mathrm{tw}}$), typical of spun MOFs, this can be achieved with elliptically polarised light.

Figure 2 presents the PS evolution results for MOFs modelled by a helical structure of their built-in linear BR axes, with elliptically polarised light at the fibre input (ellipticity angle $\varepsilon = 28^{\circ}$, $\tan\varepsilon = 0.53$). As seen, the PS does not leave the northern hemisphere, and hence a higher sensitivity would be expected in comparison with Fig. 1c. Note that, in those computations, the bending radius ($R = 3$ and 2 mm) was considerably smaller than that in Fig. 1c ($R = 6$ mm).

In this study, combining the technologies of microstructured and spun fibres, we were able to produce a sensitive miniature fibre coil with a bending radius of ~ 2.5 mm, maintaining high magnetic-field sensitivity of the coil.

The MOF was fabricated by the stack-and-draw technique and had a simple configuration, with six holes and a quasi-elliptical silica core (Fig. 3a). As shown in our previous studies, this design ensures high linear BR, up to 7×10^{-3} in the best samples. The spun MOF used in this study had the following parameters: linear BR beat length at 1550 nm $L_{\mathrm{b}} \approx 1$ mm, spin pitch $L_{\mathrm{tw}} \approx 3.5$ mm. It is worth noting that preform spinning during the drawing process slightly changed the geometry of the holes in the MOF. In particular, one of the holes was nearly collapsed (Fig. 3b). This increased the loss to ~ 0.5 dB m^{-1}, but the loss in samples produced without preform spinning was 0.01–0.03 dB m^{-1}, suggesting that this drawback can be elimi-

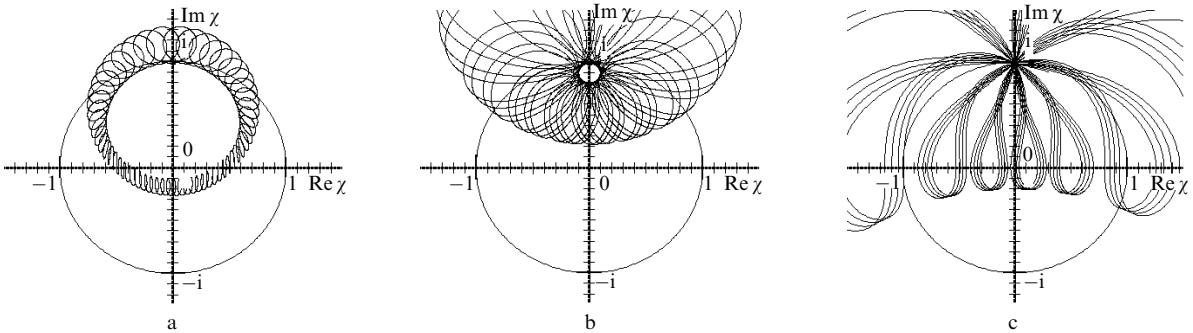

Figure 1. PS evolution in a fibre coil of radius $R = 6$ mm with a helical structure of linear BR; spin pitch $L_{\mathrm{tw}} = 3$ mm; built-in linear BR beat length $L_{\mathrm{b}} = 10$ (a) 10, (b) 3 and (c) 1 mm; right-hand circular polarisation at the fibre input. The relative magneto-optical sensitivity is $S/S_{\mathrm{id}} = 0.295$ (a), 0.74 (b), and 0.304 (c).

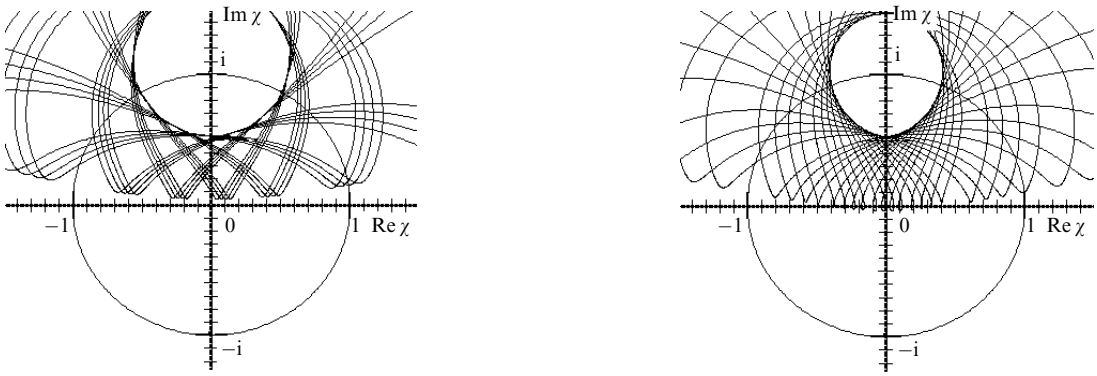

Figure 2. PS evolution in MOF coils of radius (a) 3 and (b) 2 mm; spin pitch $L_{tw} = 3$ mm, built-in linear BR beat length $L_b = 1$ mm. The relative magneto-optical sensitivity of the coils is $S/S_{id} = 0.608$ (a) and 0.581 (b). Excitation by elliptically polarised light with an ellipticity angle $\varepsilon = 28^\circ$ ($\tan\varepsilon = 0.53$).

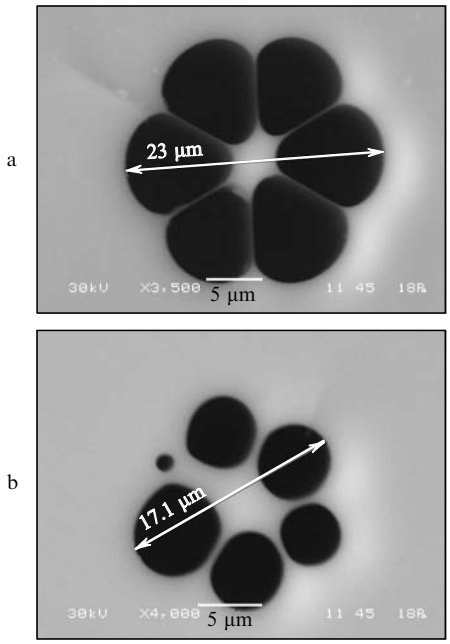

Figure 3. Cross-sectional micrographs of MOFs produced by drawing (a) without and (b) with preform spinning.

nated. An important point is that coiling our MOFs with a radius R had no effect on the loss.

Figure 4 schematically shows the experimental setup used to observe the Faraday effect in the spun MOF. The setup included a fibre-optic polarisation interferometer (FPI) [5, 8], which produced two orthogonally polarised light waves. The main components of the interferometer were a fibre-optic 1.55-μm light source (*7*), photodiode (*8*), circulator (*9*), fibre-optic polariser (*10*), piezoelectric fibre birefringence modulator (*11*) and fibre delay line (*12*). The last two elements were fabricated from polarisation-maintaining fibre. A key element of the FPI was a magnetic-field-sensitive fibre coil (*1*) of radius R, consisting of N turns of the spun MOF, with input (*3*) and output (*4*) ends. A wire (*2*) passed through the coil carried a standard electric current, I_0. We fabricated several sensing coils with various MOF winding radii, R. The output end of the coiled fibre was perpendicularly cleaved and was used as a Fresnel mirror (*5*) of the interferometer (in a number of experiments, an aluminium mirror was used). Inserted between the fibre quarter-wave plate (*6*) and the spun MOF coil were sections of conventional spun fibre and spun MOF, so the waves at the coil input had in general orthogonal elliptical polarisations. The signal processing unit (*13*) measured the amplitude of the modulation component of the current through the photodiode for subsequent calculation of the Faraday-effect-induced phase shift, φ_F.

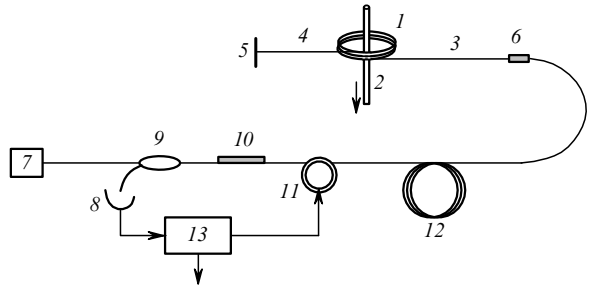

Figure 4. Schematic of the experimental setup.

The phase shift φ_F measured in the coil is related to the current by

$$\varphi_F = 4(S/S_{id})VNI_0, \tag{6}$$

where $S/S_{id} \leqslant 1$ and $V = 7\times10^{-7}$ rad A^{-1} at a wavelength of 1.55 μm.

The FPI was calibrated using a spun fibre coil with $L_b \approx 6$ mm, $L_{tw} \approx 2.5$ mm and a near-unity relative magneto-optical sensitivity. The interferometer enabled measurements of expected phase shifts ($\varphi_F \sim 1$ mrad) with an uncertainty within 3 %.

Figure 5 plots the measured relative magneto-optical sensitivity S/S_{id} against the bending radius of the spun microstructured fibre. The sensitivity is seen to be independent of R to within experimental uncertainty, with an average of 0.67 ± 0.02. Also shown in Fig. 5 is the curve computed with the same fibre parameters as in our experiments, using a model for spun fibre proposed earlier [5]. The light at the input of the fibre coil was assumed to have an elliptical polarisation.

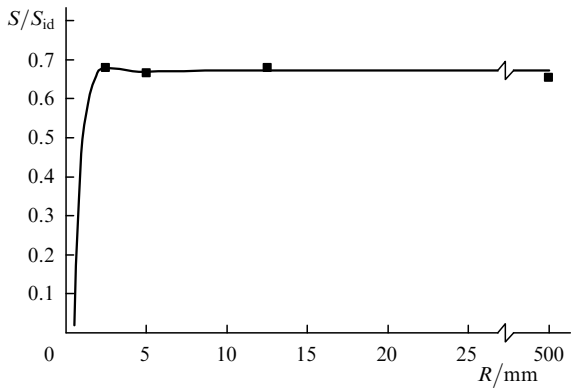

Figure 5. Measured (points) and calculated (solid line) magneto-optical sensitivity as a function of the bending radius of spun microstructured fibres.

Thus, our experiments revealed unique properties of spun MOFs. First, the measured sensitivity markedly exceeds that expected for spun MOFs with the above parameters ($L_b < L_{tw}$) under excitation with circularly polarised light. According to theoretical predictions [5], the relative sensitivity S/S_{id} of spun fibre with $L_{tw} = 3.5$ mm and $L_b = 1$ mm under such excitation is 0.3.

As mentioned above, the highest sensitivity of a spun-fibre coil with $L_b > L_{tw}$ is ensured when the waves at the coil input are circularly polarised. For the inverse relationship ($L_b < L_{tw}$), theory predicts a drop in relative sensitivity to 0.3 [5]. The present experimental results are consistent with theoretical predictions [5] if the ellipticity angle of the light launched into the coil is 22.7°, which was the case in our experiments. The light at the output of the quarter-wave plate is circularly polarised. At the same time, the polarisation of the light at the input (and at the output) of the sensing coil, after the fibre ends, differs markedly from circular one, which follows from analysis of the wave polarisation evolution in spun fibres [5] and is supported by direct measurements of the ellipticity angle at the output end of spun fibre [10, 11].

Secondly, the magneto-optical response of the spun MOF is independent of bending radius down to values as low as $R = 2.5$ mm. This can be explained by the stronger built-in linear BR, unattainable in conventional spun fibres, which suppresses the linear BR induced by small-radius bending. Note the very small scatter in sensitivity for different coil diameters.

Thus, we performed the first experimental study of the magneto-optical response of spun microstructured fibres with high built-in birefringence. The results demonstrate that such fibres enable the Faraday-effect-induced phase shift to effectively accumulate in a magnetic field even at very small coiling diameters. The use of spun MOFs enables an order of magnitude reduction in the minimum admissible bending radius compared to conventional spun fibres. In particular, the magneto-optical sensitivity of spun MOFs remains constant at $\sim 70\,\%$ of the sensitivity of an ideal fibre down to a bending radius of 2.5 mm. Our experimental data agree well with the modelling results for fibres with a helical structure of the built-in linear BR axes. Moreover, the present results suggest that spun MOFs are more promising for enhancing the magneto-optical response of current sensors than, e.g., dopants raising the Verdet constant of silica [12]. Therefore, spun MOFs can be used to fabricate miniature fibre coils consisting of 10^3 to 10^4 turns for high-performance current sensors.

Acknowledgements. We are grateful to G.A. Ivanov and V.V. Voloshin for their valuable assistance with this study. This work was supported by the Presidium of the Russian Academy of Sciences (Programme Nos P-2 and P-21).

References

1. Ortigosa-Blanche A., Knight J.C., Wadsworth W.J., Arringe J., Mangan B.J., Birks T.A., Russell P.St.J. *Opt. Lett.*, **25**, 1326 (2000).
2. Michie A., Canning J., Lyytikainen K., Aslung M., Digweed J. *Opt. Express*, **21**, 5160 (2004).
3. Laming R.I., Payne D.N. *J. Lightwave Technol.*, **7**, 2084 (1989).
4. Polinkin P., Blake J. *J. Lightwave Technol.*, **23**, 3815 (2005).
5. Gubin V.P., Isaev V.A., Morshnev S.K., Sazonov A.I., Starostin N.I., Chamorovsky Yu.K., Oussov A.I. *Kvantovaya Elektron.*, **36**, 287 (2006) [*Quantum. Electron.*, **36**, 287 (2006)].
6. Rashleigh S.C. *J. Lightwave Technol.*, **1**, 312 (1983).
7. Azzam R.M.A., Bashara N.M. *Ellipsometry and Polarized Light* (Amsterdam – New York – Oxford: North-Holland Publ. Comp., 1977).
8. Bohnert K., Gabus P., Nehring J., Brändle H. *J. Lightwave Technol.*, **20**, 267 (2002).
9. Morshnev S.K., Gubin V.P., Vorob'ev I.L., Starostin N.I., Sazonov A.I., Chamorovsky Yu.K., Korotkov N.M. *Kvantovaya Elektron.*, **39**, 287 (2009) [*Quantum. Electron.*, **39**, 287 (2009)].
10. Michie A., Canning J., Bassett J., Haywood J., Digweed K., Aslung M., Ashton B., Stevenson M., Digweed J., Lau A., Scandurra D. *Opt. Express*, **15**, 1811 (2007).
11. Gubin V.P., Morshnev S.K., Starostin N.I., Sazonov A.I., Chamorovsky Yu.K., Isaev V.A. *Radiotekh. Elektron.*, **53**, 971 (2008).
12. Watekar P.R., Yang Hououng, Ju Seongmin, Han Won-Taek. *Opt. Exspress*, **17** (5), 3157 (2009).